

# Decadal variance of summer near-surface temperature maximum in Canada Basin of Arctic Ocean

By LONG LIN<sup>1,2</sup> and HAILUN HE<sup>1\*</sup>, <sup>1</sup>*State Key Laboratory of Satellite Ocean Environment Dynamics, Second Institute of Oceanography, Ministry of Natural Resources, Hangzhou, China;*  
<sup>2</sup>*Physical Oceanography Lab, Ministry of Education, Qingdao, China*

(Manuscript received 29 November 2018; in final form 2 March 2019)

## ABSTRACT

In the summer Arctic, bump-like vertical temperature profiles of the upper layer in the Canada Basin suggest a near-surface temperature maximum (NSTM) beneath the mixed layer. This paper concentrates on describing the decadal variance of these NSTMs. Essentially, the temporal evolution of the summer NSTM revealed three decadal phases. The first period is before 2003, when the summer NSTM could rarely be observed except around the marginal of the Canada Basin. The second period is between 2003 and 2015, when the summer NSTM nearly occurred over the whole basin as accelerated decline of summer sea ice. The third period is from 2016 to 2017, when the summer NSTM almost disappeared due to prevailing warm surface water. Furthermore, for the background behind the decadal variance of summer NSTM, linear trends of the September minimum sea ice extent and surface water heat content in the Canada Basin from 2003 to 2017 were  $-2.75 \pm 1.08 \times 10^4 \text{ km}^2 \text{ yr}^{-1}$  and  $2.29 \pm 1.36 \text{ MJ m}^{-2} \text{ yr}^{-1}$ , respectively. According to a previous theory, if we assume that the trend of the summer surface water heat content was only contributed by NSTM, it would cause a decrease in sea ice thickness of approximately 13 cm. The analysis partially explains the reason for sea ice decline in recent years.

*Keywords:* near-surface temperature maximum, heat content, Canada Basin, Arctic Ocean

## 1. Introduction

In the Canada Basin of the Arctic Ocean, there are usually two distinct temperature maximums at the depth of 60–80 m and 300–600 m, which represented the Pacific Summer Water (PSW) and the Atlantic Water (AW), respectively (Aagaard et al., 1985; Shimada et al., 2005; Timmermans et al., 2014; Zhong and Zhao, 2014). While another temperature maximum named near-surface temperature maximum (NSTM), between the mixed layer and PSW, has caused great concern under the background of Arctic warming (Maykut and McPhee, 1995; McPhee et al., 1998; Jackson et al., 2010; Steele et al., 2011). NSTM forms when sufficient solar radiation warms the upper ocean. Due to the exponential decaying, most of the solar energy is devoted to sea ice melting and mixed-layer heating, while a portion of solar energy still can be stored just below the mixed layer and trapped by strong stratification (related to summer halocline) after sea ice melts. NSTM keeps below summer halocline until sufficient brine rejection-induced penetrative convection

and surface stress extending the mixed layer (Jackson et al., 2010). Surface cooling and solar heating were proposed as two fundamental conditions of the NSTM formation mechanism (Zhao and Cao, 2012).

In essential, NSTM comprises the dynamic and thermodynamic links between sea ice and underlying water (Steele et al., 2011; Jackson et al., 2012; Shen et al., 2018). The solar energy stores in the NSTM when sea ice melts during summertime, and then entrained into the mixed layer and contributes to the sea ice bottom by the diffusion or erosion of the summer halocline in freezing season (Jackson et al., 2012; Timmermans, 2015; Lin and Zhao, 2019). The heat released from NSTM slows down the sea ice growth rate and impedes surface layer deepening, which limits the flux of deeper ocean heat to the surface (Toole et al., 2010). In other words, the impacts of NSTM on Arctic are represented from at least three aspects. Firstly, NSTM warms the upper ocean by trapping solar energy under mixed layer in summertime. Secondly, NSTM strengthens the stratification of the upper ocean as a barrier layer, which limits the vertical convection and momentum transfer. Thirdly, the heat

\*Corresponding author. e-mail: [hehailun@sio.org.cn](mailto:hehailun@sio.org.cn)

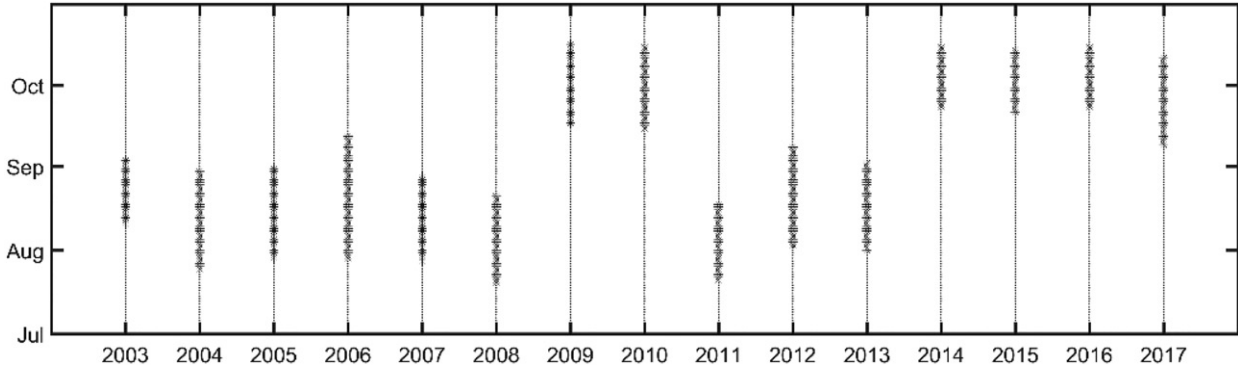


Fig. 1. LSSL expedition time during 2003 to 2017.

release from NSTM delays autumn freeze-up and affects sea ice recovery. So the NSTM plays considerable roles in the coupled atmosphere-ice-ocean system in Arctic.

The accelerated retreat of both sea ice extent (Cavaliere and Parkinson, 2012; Vihma, 2014; Serreze and Meier, 2018) and thickness (Kwok and Rothrock, 2009; Kwok and Untersteiner, 2011; Laxon et al., 2013) increases greater absorption of solar radiation in the upper ocean (Perovich et al., 2007; Toole et al., 2010; Stroeve et al., 2014). As a result, NSTM has warmed and freshened by approximately  $1.5^{\circ}\text{C}$  and 4 psu, respectively, from 1993 to 2009 and the depth of NSTM shoaled by  $2.1 \text{ myr}^{-1}$  from 1997 to 2007 (Jackson et al., 2010, 2011). According to Jackson et al. (2010), there are also some interannual signals in NSTM temperature. For instance, NSTM temperature was the highest in 2007 for north of  $75^{\circ}\text{N}$ , and the minimum temperature occurred in either 2003 or 2004. In addition, for spatial variation, the observed NSTM expanded north from marginal seas and became a common feature in the whole Canada Basin especially after 2003 (Zhao and Cao, 2012). While, despite these documented NSTM changes, very little is known about how the NSTM would change with the continuous decline of sea ice, especially after 2012 (lowest recorded summer sea ice extent) (Parkinson and Comiso, 2013). The exact relationship between the summer NSTM and sea ice conditions is still unclear and needs to be quantified. Furthermore, the heat content of the summer NSTM should be analyzed in combination with surface water.

Therefore, the objective of this paper stands on the following questions: (1) What properties of NSTM are affected under different sea ice condition? (2) How has the summer NSTM changed since the dramatic decline of sea ice from 2003, especially in 2012, 2016 and 2017? Here, we explore the decadal variation of summer NSTM and the changes of the surface water from the 1990s to 2017 based on the historical conductivity, temperature and depth surveys.

The structures of this paper are organized as follows: Section 2 represents the data description, Section 3 addresses the description of the summer NSTM, decadal variance of NSTM and the trend of the surface water heat content in the central Canada Basin, and the conclusion is drawn in Section 4.

## 2. Data

A basin-wide conductivity, temperature and depth (CTD) database of the Canada Basin in the Arctic Ocean from 2003 to 2017 was collected by the Canadian Coast Guard Icebreaker Louis S. St-Laurent (LSSL) and issued by the Joint West Arctic Climate Study (JWACS) and Beaufort Gyre Exploration Project (BGEP). The yearly observation times of the LSSL are shown in Fig. 1. The expeditions were mainly conducted in August and September from 2003 to 2017. Section CTD data in 1996 and 1997 refer to the World Ocean Database 2013 issued by the Ocean Climate Laboratory of the National Oceanographic Data Center. Sea ice concentrations were derived from Advanced Microwave Scanning Radiometer-EOS brightness temperatures, with a resolution of  $6.25 \times 6.25 \text{ km}$  (Spreen et al., 2008). Representative sea ice concentrations during the ship-based CTD sampling were estimated within circles of 100 km radii (Stanton et al., 2012), and local wind speeds were derived from NCEP/NCAR reanalysis (Kistler et al., 2001).

## 3. Results

### 3.1. Description of the summer NSTM from 2003 to 2017

According to the definition of the NSTM by Jackson (Jackson et al., 2010), yearly summer NSTM were identified from CTD measurements from 2003 to 2017. The most striking feature is that almost all NSTMs were observed under sea ice cover (Fig. 2). Some NSTMs were even

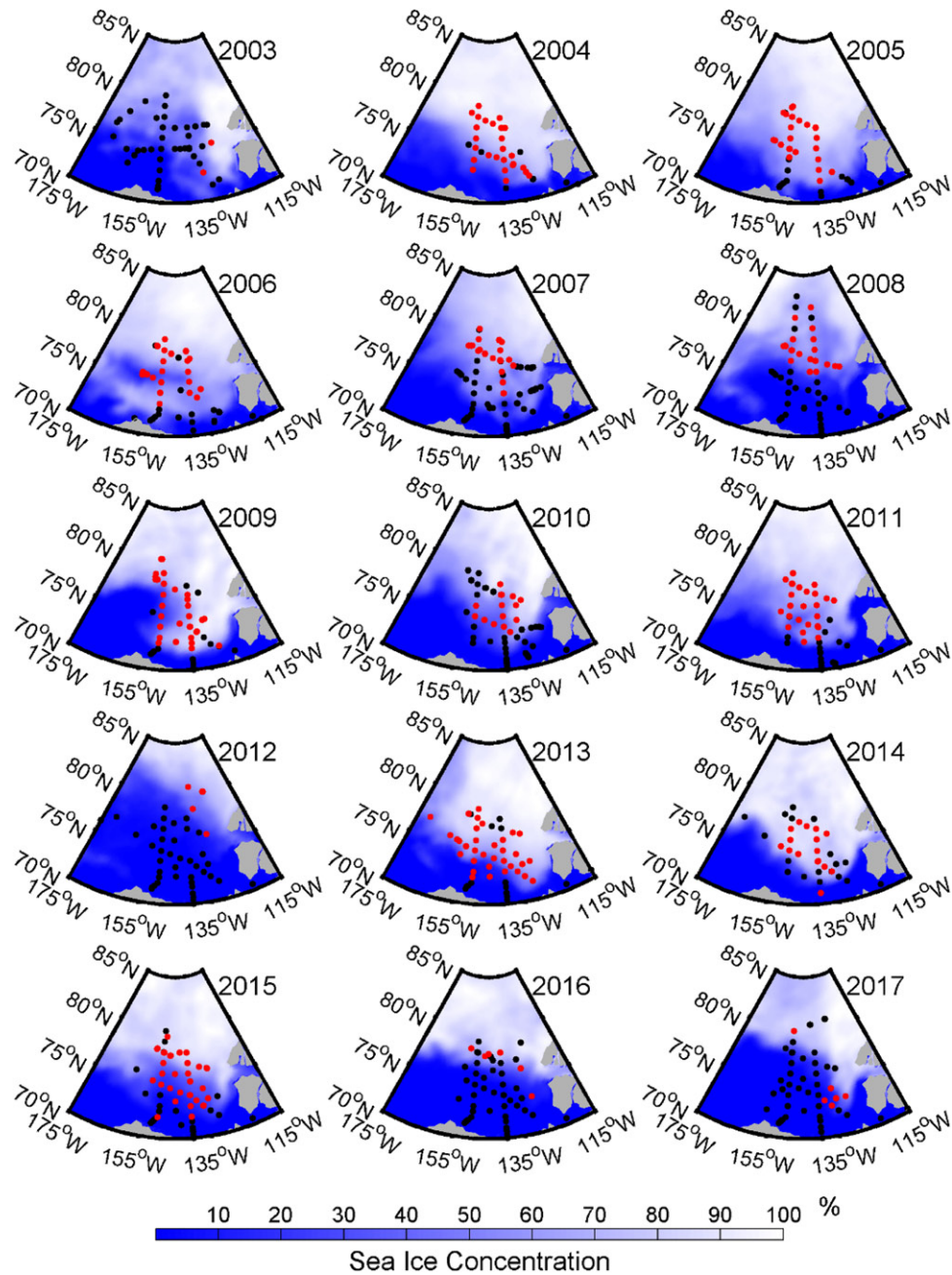


Fig. 2. Distribution of summer NSTM during 2003–2017. Red dots represent the stations where NSTM existed, while black dots represent the stations without NSTM. The background represents the mean sea ice concentration during the expedition time.

observed north of 80°N in 2008, 2009 and 2012. Meanwhile, NSTM is hardly observed in open water. This feature conforms to the known mechanics of NSTM formation.

Sea ice influences the formation of NSTM from two aspects. On the one hand, the existence of sea ice provides the condition of surface cooling, which maintains the mixed layer temperature near freezing point but lower than the near-surface temperature maximum. On

the other hand, the heat in NSTM comes from the solar energy entering the upper ocean through open water and leads or penetrates through the sea ice column during sea ice melting. Once the sea ice melts out totally, surface cooling cannot be maintained. Then, NSTM disappeared in open water. This is the reason why the spatial NSTM changes with the sea ice edge.

The spatial distribution of the NSTM temperature is presented in Fig. 3. The distinct common feature is that

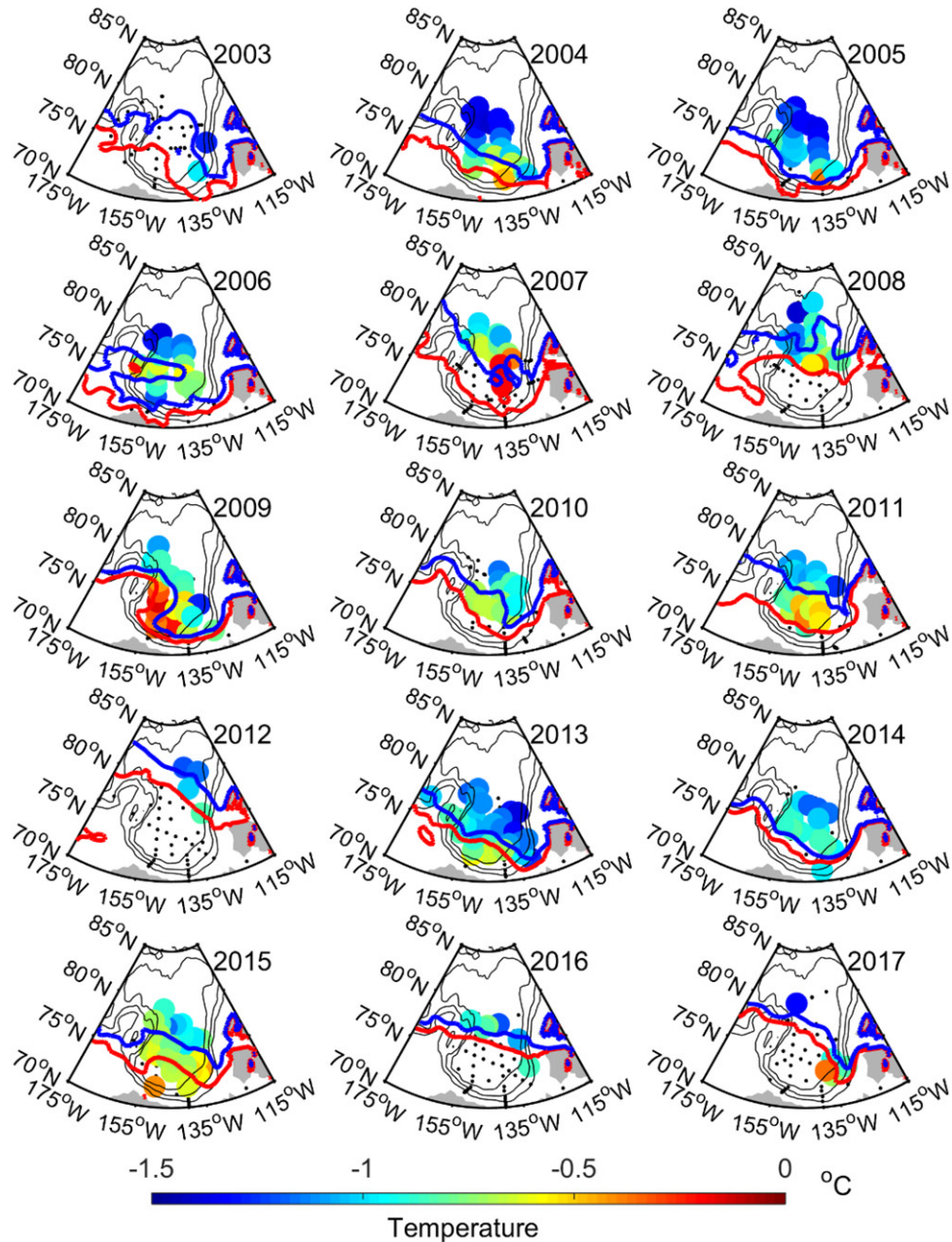


*Fig. 3.* Distributions of the summer NSTM temperature. Shaded circles represent the NSTM temperature, and black dots indicate the CTD stations without NSTM. The red line displays the contour of 15% sea ice concentration (sea ice edge), and the blue line is for 50% sea ice concentration.

the temperature of NSTM in marginal sea ice zone was much higher than that in pack ice cover. If we classified sea ice into marginal ice zone with sea ice concentration of 15% to 50% and pack ice cover with sea ice concentration larger than 50%, our results support that the mean temperature of summer NSTM in marginal ice zone ( $-0.65^{\circ}\text{C}$ ) was nearly  $0.3^{\circ}\text{C}$  higher than that in pack ice cover ( $-0.96^{\circ}\text{C}$ ). The reason was that the upper ocean of marginal ice zone received more efficient solar energy due

to lower sea ice concentration and also had stronger stratification than that in pack ice cover.

In addition, heat content is an important index for heat energy. The heat content (HC) of summer NSTM was calculated relative to the freezing point from 10 m to the depth of the remnant of winter mixed layer (rML, a residual from the previous winter mixed layer after seasonal restratification). The spatial distributions of the summer NSTM HC are presented in [Fig. 4](#). The spatial

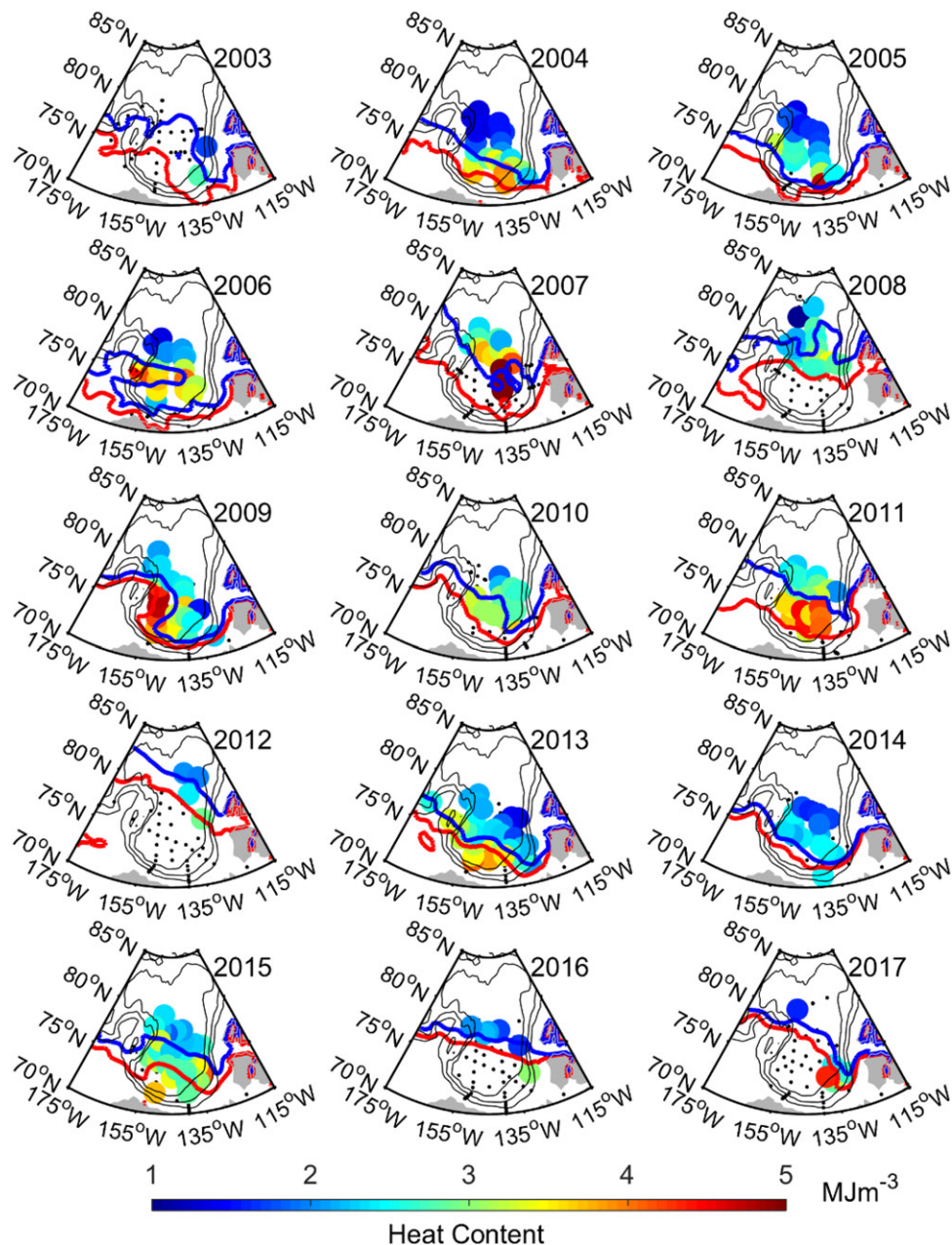


Fig. 4. Distributions of the summer NSTM heat content. Shaded circles represent the NSTM heat content, and black dots indicate the CTD stations without NSTM. The red line displays the contour of the 15% sea ice concentration (sea ice edge), and the blue line is for 50% sea ice concentration.

variations of NSTM HC were well consistent with summer NSTM temperature. Since the summer NSTM HC was mainly controlled by the maximum temperature and the depth of rML, a NSTM with higher temperature always corresponds to higher heat content, and vice versa. Corresponding to the aforementioned temperature, the summer NSTM HC was 3.45 and 2.53  $\text{MJm}^{-3}$  in marginal ice zone and pack ice cover, respectively. It is notable that our estimation is slightly larger than that

observed by the Ice-Tethered Profilers (ITP) under pack ice (Jackson et al., 2010). We speculate that ITP underestimated the heat in the summer NSTM because historical ITPs were always deployed on thick ice.

For the formation and development of NSTM, sea ice concentration, Julian day, latitude and wind are suggested as potential factors for the observed summer NSTM (i.e. the melting of sea ice and the annual cycle of solar radiation). Figure 5 shows the correlations of the summer

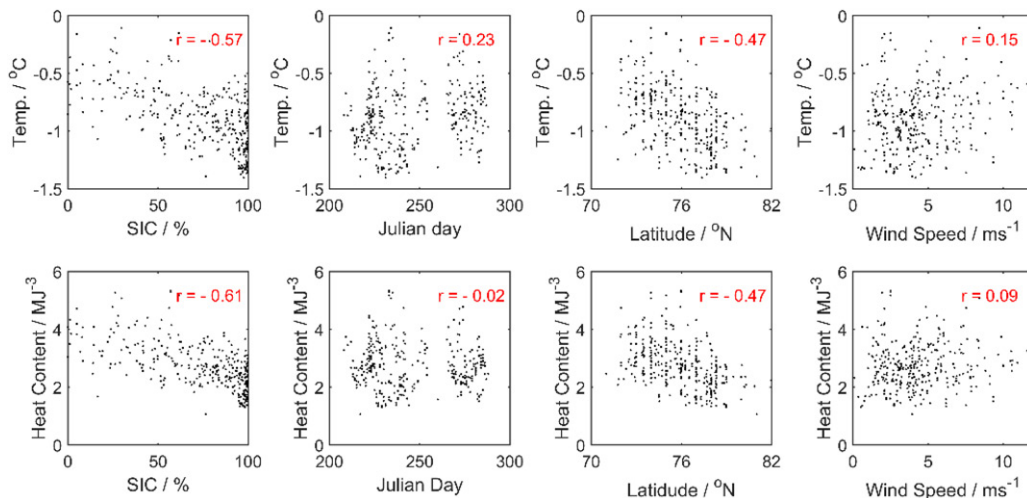


Fig. 5. The relationship of the summer NSTM temperature and heat content with sea ice concentration (SIC), Julian day, latitude, and wind speed.

NSTM properties with these four factors. For the overall observed NSTM from 2003 to 2017, the temperature of summer NSTM has good correlations with the sea ice concentration and latitude ( $r = -0.57$ ,  $p < 0.001$ , and  $r = -0.47$ ,  $p < 0.001$ , respectively;  $r$  is correlation coefficient, and  $p$  is corresponding confidence interval value) but poor correlation with Julian day and local wind speed ( $r = 0.23$ ,  $p < 0.001$ ;  $r = 0.15$ ,  $p < 0.01$ ). Similar results were obtained for the relationships between the NSTM HC and sea ice concentration, Julian day, latitude and wind speed, with correlation coefficients of  $-0.61$  ( $p < 0.001$ ),  $-0.02$  ( $p > 0.5$ ),  $-0.47$  ( $p < 0.001$ ) and  $0.09$  ( $p > 0.09$ ), respectively. Generally, the sea ice concentration was larger and solar energy was weaker at higher latitudes than that at lower latitudes, which means that less solar energy entered the upper ocean. This was the reason why the summer NSTM in higher latitude was colder than that at lower latitude. Meanwhile, for a single NSTM, there was no doubt that the properties of NSTM change with time. However, the temporal evolution (or Julian day dependence) is somewhat covered in the seasonal studies. In addition, the connection between NSTM and wind is relatively weak due to the isolation effect of sea ice.

### 3.2. Decadal variance of NSTM

Due to the rapid decline of summer sea ice concentration in the Canada Basin from the 20th to 21st centuries, the summer NSTM also experienced significant change. Considering the consistency in the observation time, the meridional September temperature sections in the upper Canada Basin in 1996, 1997, 2009, 2010, 2016 and 2017 are shown in Fig. 6. Based on the temporal variation of summer NSTM, we can roughly divide 22 years into three

periods: before 2003, from 2003 to 2015 and from 2016 to 2017.

First, before 2003, the summer sea ice was relatively thick and dense in the Canada Basin, and most of the downward solar energy was reflected by snow and sea ice due to high albedo. Therefore, only a small amount of solar energy could enter the upper ocean, and almost all of it totally contributed to the sea ice bottom. As a result, there was hardly any NSTM in the central Canada Basin (Fig. 6a and b), but some of the NSTM existed around the marginal of the basin (Zhao and Cao, 2012).

Second, from 2003 to 2015, as the sea ice concentration and thickness decreased, solar energy effectively entered the upper ocean through open water and leads or penetrated through the thinner sea ice column. Most of the solar energy transformed into oceanic heat flux, contributing to the sea ice bottom melt and maintaining the temperature of mixed layer slightly above the freezing point. The rest was trapped under the summer halocline at a depth of 20 to 30 m, forming a summer NSTM with a maximum temperature of  $0.66^\circ\text{C}$  on average above the freezing point (Fig. 6c and d). In most years (except 2003), NSTM almost existed wherever there was sea ice cover, from marginal ice zone to pack ice cover, and even reached north of  $80^\circ\text{N}$  in 2008 and 2009 (Fig. 2). Therefore, the melting of sea ice promoted the formation of summer NSTM.

Third, in 2016 and 2017, (and also in 2012), sea ice melted heavily, and the sea ice edge retreated north of  $75^\circ\text{N}$  in the Canada Basin, as did the summer NSTM. Once the sea ice melted out entirely and became open water in the southern Canada Basin, NSTM disappeared. Because continuous solar heating and mixing progress warmed the surface layer, a clear temperature difference

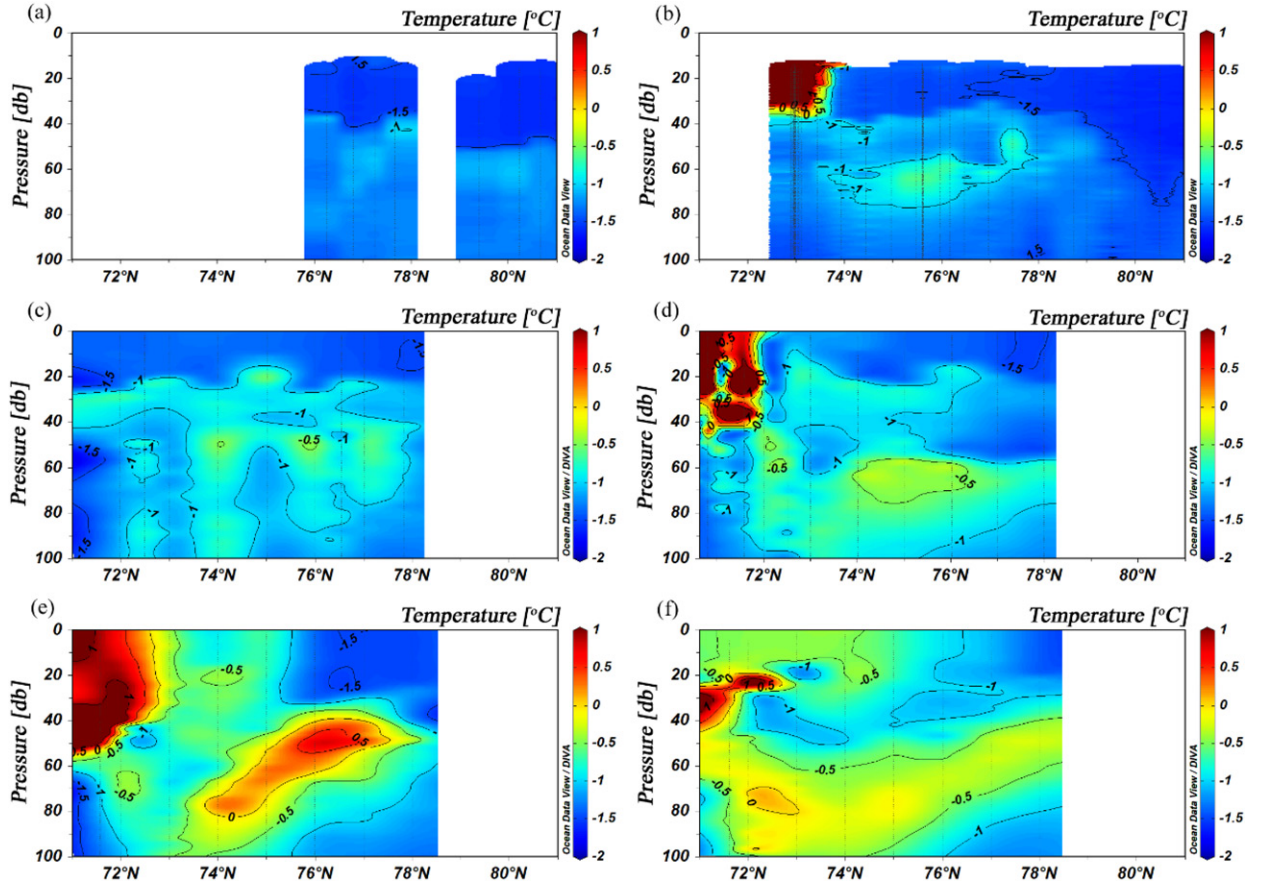


Fig. 6. Meridional September temperature sections in the upper ocean of the Canada Basin. (a) 1996, (b) 1997, (c) 2009, (d) 2010, (e) 2016, (f) 2017. Sections (b), (c), (d), (e) and (f) were located along  $140^{\circ}\text{W}$ , while section (a) was slightly slanted.

between the mixed layer and NSTM formed early and became indistinct (Fig. 6e and f). As there was no surface cooling, NSTM structure was destroyed, and warm surface water prevailed.

As a consequence, NSTM is a transient phenomenon under the background of Arctic warming. It cannot form without sufficient solar energy entering the upper ocean with dense sea ice. A decrease in sea ice concentration and the thinning of sea ice thickness allows greater absorption of solar energy in the upper ocean, promoting the formation of NSTM. We are currently experiencing the prevalence of NSTM. In fact, NSTM is similar to a ‘parasite’ on sea ice. Once sea ice melts out, it is difficult to maintain the condition of surface cooling. This is why NSTM disappeared, especially in 2012, 2016 and 2017, when sea ice melted heavily.

### 3.3. Surface water heat content in the Central Canada Basin

Because the summer NSTM varied with sea ice cover change, the summer NSTM HC could not represent the annual changes of the upper oceanic heat content. Thus,

we restricted the oceanic heat content in the upper (10–40 m) Central Canada Basin (CCB) within  $79^{\circ}\text{N}$ ,  $150^{\circ}\text{W}$ ,  $74^{\circ}\text{N}$  and  $135^{\circ}\text{W}$ . The annual mean heat content in the upper CCB from 2003 to 2017 is represented in Fig. 7. The heat content in the CCB showed an increasing trend of  $2.29 \pm 1.36 \text{ MJm}^{-2}\text{yr}^{-1}$ . The total heat content increment in this period was  $34.35 \text{ MJm}^{-2}$ . If all of this heat was gradually released to the cooling atmosphere before any ice formed, it implied an autumn freeze-up delay of  $\Delta t = \Delta H C / (\rho_{\text{air}} c_{p,\text{air}} c_{h,\text{aw}} \Delta T_{\text{aw}} W_{10\text{m}}) = 3\text{--}12$  days, where the air density is  $\rho_{\text{air}} = 1.3 \text{ kgm}^{-3}$ , the air heat capacity is  $c_{p,\text{air}} = 103 \text{ Jkg}^{-1}\text{C}^{-1}$ , the air water heat exchange coefficient is  $c_{h,\text{aw}} = 10^{-3}$ , and we assume an air–water temperature difference of  $\Delta T_{\text{aw}} = 5\text{--}10^{\circ}\text{C}$  and a 10 m elevation wind speed of  $W_{10\text{m}} = 5\text{--}10 \text{ ms}^{-1}$  (Steele et al., 2008). If all of this heat was released during freezing, it would reduce the total sea ice thickness of 13 cm.

We also calculate the September minimum sea ice extent in the Canada Basin within  $82^{\circ}\text{N}$ ,  $160^{\circ}\text{W}$ ,  $70^{\circ}\text{N}$  and  $120^{\circ}\text{W}$  in the same period (Fig. 7). The results show a decreasing trend of  $-2.75 \pm 1.08 \times 10^4 \text{ km}^2\text{yr}^{-1}$ . The heat content in the upper CCB and the September

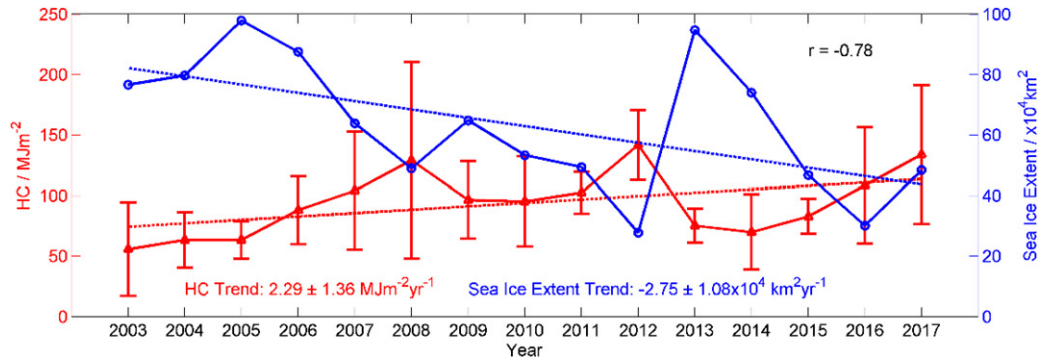


Fig. 7. Linear trend of HC in the CCB (red) and September minimum sea ice extent in the Canada Basin (blue).

minimum sea ice extent in the Canada Basin had a good negative relationship with a correlation coefficient of  $-0.78$  ( $p < 0.001$ ). It follows that a decrease in summer sea ice extent would result in more solar heat being deposited in the upper ocean and an increase melting. This positive feedback accelerated the decline of Arctic sea ice cover. Besides, it is worthy noted that the relationship between heat content and summer Arctic Oscillation (AO, June–October) index is relatively weak ( $r = 0.29$ ; not shown here).

#### 4. Conclusion

In this paper, we mainly focus on the sea ice dependence of the summer NSTM and its decadal variance in the Canada Basin of the Arctic Ocean. NSTM did not exist throughout the summer in the whole basin, but relied on solar heating and surface cooling.

Both solar heating and surface cooling are related to the sea ice concentration. As a result, both the temperature and heat content of NSTM had a good relationship with the sea ice concentration. Therefore, we classified sea ice into marginal ice zone and pack ice cover and then explored the properties of the summer NSTM under different sea ice conditions. The mean temperature of summer NSTM in the marginal ice zone was  $-0.65^{\circ}\text{C}$ , while that in pack ice cover was  $-0.96^{\circ}\text{C}$ . The vertical mean summer NSTM heat content from 10 m to the depth of the remnant of the winter mixed layer was  $3.45 \text{ MJm}^{-3}$  in marginal ice zone and  $2.53 \text{ MJm}^{-3}$  in pack ice cover, with a total average value of  $2.72 \text{ MJm}^{-3}$ . The heat of NSTM was released to the base of the sea ice via erosion of the summer halocline during the freezing season. If all of the heat in NSTM was completely released, it would cause a decrease in winter ice growth of 30 cm.

NSTM shows clear decadal variance. From 2003 to 2017, compared with the 1990s, the results reveal that the decline of sea ice promoted the formation of NSTM from

the marginal to the central Canada Basin and even north of  $80^{\circ}\text{N}$ . While in extreme years such as 2012, 2016 and 2017, the sea ice totally melted and turned into open water in the southern part of the Canada Basin. Then, continuous solar heating of the upper ocean destroyed the NSTM maintaining condition of surface cooling. As a result, NSTM disappeared, and warmer surface water prevailed. In other words, the NSTM is simply a transient phenomenon in the sea ice melting process.

Based on basin-wide CTD data, we have the capability to compute the general trend of the surface water heat content in the central Canada Basin from 2003 to 2017. The results show a clear increasing trend of  $2.29 \pm 1.36 \text{ MJm}^{-2}\text{yr}^{-1}$ . Moreover, the interannual variance of the surface water heat content in the Canada Basin has a good relationship with the September minimum sea ice extent. Actually, we can divide the surface water heat content into two parts: the heat content in the mixed layer and the heat content of NSTM. The heat content in the mixed layer releases before freezing in autumn, resulting in a freeze-up delay, while the heat content in NSTM releases during freezing season, causing a decrease in sea ice growth. In terms of discussion, if we assume that the heat content of the mixed layer was negligible and the trend of surface water heat content was contributed by NSTM, these heat increases would cause an ice thickness decrease of 13 cm. This result does not deviate substantially from reality which, to some extent, could explain the low-frequency variation of sea ice.

#### Acknowledgements

The authors are grateful to Beaufort Gyre Exploration Project for their efforts in collecting and pre-processing CTD data. Thanks also due to the University of Bremen for their sea ice concentration products. The graphics were generated using the Matlab and Ocean Data View



(ODV). Comments and suggestions provided by anonymous reviewers are greatly appreciated.

## Disclosure statement

No potential conflict of interest was reported by the authors.

## Funding

This work was supported by the National Basic Research Program of China (Grant No. 2015CB953900), the National Natural Science Foundation of China (Grant No. 41621064), and the polar consulting project of Chinese Academy of Engineering (Grant No. 2018-XZ-12-02).

## References

- Aagaard, K., Swift, J. H. and Carmack, E. C. 1985. Thermohaline circulation in the Arctic Mediterranean Sea. *J. Geophys. Res.* **90**, 4833–4846. doi:10.1029/JC090iC03p04833
- Cavalieri, D. J., and Parkinson, C. L. 2012. Arctic sea ice variability and trends, 1979–2010. *The Cryosphere*. **6**, 881–889. doi:10.5194/tc-6-881-2012
- Jackson, J. M., Allen, S. E., McLaughlin, F. A., Woodgate, R. A. and Carmack, E. C. 2011. Changes to the near-surface waters in the Canada Basin, Arctic Ocean from 1993–2009: A basin in transition. *J. Geophys. Res. Oceans*. **116**, C10008. doi:10.1029/2011JC007069
- Jackson, J. M., Carmack, E. C., McLaughlin, F. A., Allen, S. E. and Ingram, R. G. 2010. Identification, characterization, and change of the near-surface temperature maximum in the Canada Basin, 1993–2008. *J. Geophys. Res.* **115**, C05021.
- Jackson, J. M., Williams, W. J. and Carmack, E. 2012. Winter sea-ice melt in the Canada Basin, Arctic Ocean. *Geophys. Res. Lett.* **39**, L03603.
- Kistler, R., Collins, W., Saha, S., White, G., Woollen, J. and co-authors. 2001. The NCEP-NCAR 50-year reanalysis: Monthly means CD-ROM and documentation. *Bull. Amer. Meteor. Soc.* **82**, 247–268. doi:10.1175/1520-0477(2001)082<0247:TNNYRM>2.3.CO;2
- Kwok, R. and Rothrock D. A. 2009. Decline in Arctic sea ice thickness from submarine and ICESat records: 1958–2008. *Geophys. Res. Lett.* **36**, L15501.
- Kwok, R. and Untersteiner, N. 2011. The thinning of Arctic sea ice. *Phys. Today*. **64**, 36–41. April, doi:10.1063/1.3580491
- Laxon, S. W., Giles, K. A., Ridout, A. L., Wingham, D. J., Willatt, R., and co-authors. 2013. CryoSat-2 estimates of Arctic sea ice thickness. *Geophys. Res. Lett.* **40**, 732–737. doi:10.1002/grl.50193
- Lin, L., and Zhao, J. 2019. Estimation of oceanic heat flux under sea ice in arctic ocean. *J. Ocean Univ. China*, in press.
- Maykut, G. A. and McPhee, M. G. 1995. Solar heating of the Arctic mixed layer. *J. Geophys. Res.* **100**, 24691–24704. doi:10.1029/95JC02554
- McPhee, M. G., Stanton, T. P., Morison, J. H. and Martinson, D. G. 1998. Freshening of the upper ocean in the Arctic: Is perennial sea ice disappearing? *Geophys. Res. Lett.* **25**, 1729–1732. doi:10.1029/98GL00933
- Parkinson, C. L. and Comiso, J. 2013. On the 2012 record low Arctic sea ice cover: Combined impact of preconditioning and an August storm. *Geophys. Res. Lett.* **40**, 1356–1361. doi:10.1002/grl.50349
- Perovich, D. K., Light, B., Eicken, H., Jones, K. F., Runciman, K. and co-authors. 2007. Increasing solar heating of the Arctic Ocean and adjacent seas, 1979–2005: Attribution and role in the ice-albedo feedback. *Geophys. Res. Lett.* **34**, L19505. doi:10.1029/2007GL031480
- Serreze, M. C. and Meier, W. N. 2018. The Arctic's sea ice cover: Trends, variability, predictability, and comparisons to the Antarctic. *Ann. NY Acad. Sci.* **1436**, 36–53.
- Shen, H., Perrie, W., Hu, Y. and He, Y. 2018. Remote sensing of waves propagating in the marginal ice zone by SAR. *J. Geophys. Res. Oceans*. **123**, 189–200. doi:10.1002/2017JC013148
- Shimada, K., Itoh, M. and Nishino, S. 2005. Halocline structure in the Canada Basin of the Arctic Ocean. *Geophys. Res. Lett.* **32**, L03605.
- Spreen, G., Kaleschke, L. and Heygster, G. 2008. Sea ice remote sensing using AMSR-E 89 GHz channels. *J. Geophys. Res.* **113**, C02S03.
- Stanton, T., Shaw, W. J. and Hutchings, J. K. 2012. Observational study of relationships between incoming radiation, open water fraction. *J. Geophys. Res.* **117**, C07005.
- Steele, M., Ermold, W. and Zhang, J. 2008. Arctic Ocean surface warming trends over the past 100 years. *Geophys. Res. Lett.* **35**, L02614.
- Steele, M., Ermold, W. and Zhang, J. 2011. Modeling the formation and fate of the near-surface temperature maximum in the Canadian Basin of the Arctic Ocean. *J. Geophys. Res.* **116**, C11015. doi:10.1029/2010JC006803
- Stroeve, J. C., Markus, T., Boisvert, L., Miller, J. and Barrett, A. 2014. Changes in Arctic melt season and implications for sea ice loss. *Geophys. Res. Lett.* **41**, 1216–1225. doi:10.1002/2013GL058951
- Timmermans, M. L. 2015. The impact of stored solar heat on Arctic sea ice growth. *Geophys. Res. Lett.* **42**, 6399–6406. doi:10.1002/2015GL064541
- Timmermans, M. L., Proshutinsky, A., Golubeva, E., Jackson, J. M., Krishfield, R., and co-authors. 2014. Mechanisms of Pacific Summer Water variability in the Arctic's Central Canada Basin. *J. Geophys. Res. Oceans*. **119**, 7523–7548. doi:10.1002/2014JC010273
- Toole, J. M., Timmermans, M. L., Perovich, D. K., Krishfield, R. A., Proshutinsky, A., and Richter-Menge, A. 2010. Influences of the ocean surface mixed layer and thermohaline stratification on Arctic Sea ice in the central Canada Basin. *J. Geophys. Res.* **115**, C10018. doi:10.1029/2009JC005660
- Vihma, T. 2014. Effects of Arctic sea ice decline on weather and climate: A review. *Surv. Geophys.* **35**, 1175–1214. doi:10.1007/s10712-014-9284-0
- Zhao, J. and Cao, Y. 2012. Summer water temperature structures in upper Canada Basin and their interannual variation. *Adv. Polar Sci.* **22**, 4: 223–234.
- Zhong, W. and Zhao, J. J. 2014. Deepening of the Atlantic water core in the Canada Basin in 2013–11. *J. Phys. Oceanogr.* **44**, 2353–2368. doi:10.1175/JPO-D-13-084.1